

82
AMMRC TR 81-53

Watertown, Massachusetts 02172

AD A 112054

DETERMINATION OF STRUCTURAL RELIABILITY USING A FLAW SIMULATION SCHEME

DONALD M. NEAL and DONALD S. MASON
MECHANICS OF MATERIALS DIVISION

October 1981

Approved for public release; distribution unlimited.

ARMY MATERIALS AND MECHANICS RESEARCH CENTER
Watertown, Massachusetts 02172

The findings in this report are not to be construed as an official Department of the Army position, unless so designated by other authorized documents.

Mention of any trade names or manufacturers in this report shall not be construed as advertising nor as an official indorsement or approval of such products or companies by the United States Government.

DISPOSITION INSTRUCTIONS

Destroy this report when it is no longer needed.
Do not return it to the originator.

Block No. 20

ABSTRACT

This paper describes structural reliability developed from an assumed flaw simulation scheme combined with an idealized linear elastic fracture mechanics model. In the reliability computation, it has been demonstrated that application of this scheme can provide a sensitivity analysis in relation to flaw detection capabilities. To demonstrate the versatility of the method, reliability numbers were obtained for both a simply loaded fragmentation shell and an antitank projectile subjected to a complex stress state. The flaw simulation scheme results are compared to corresponding reliability determinations from conventional Weibull and Warner stress-strength diagram methods.

The reliability definitions associated with the scheme require a probability density function representation of the material strength and stress distributions for each structural element. A density function representation of the allowable stress (strength) is obtained from fracture mechanics K_{IC} relationships in conjunction with the Monte Carlo method where a specific random form of the parameter is assigned. Crack orientations are assumed to vary in a uniform random manner with respect to the principal axis and its normal. The crack size variation is defined in exponential functional form where the sizes vary from a large number of very small cracks to a relatively small number of larger cracks. The structural configuration determines the type of crack and its location. It is assumed that flaws exist in the structural elements and are remote from any other flaws. A normal density function represented element stress variability where the mean stress was obtained from an axisymmetric analysis using a unique finite element code. Perturbations of the coefficient of variation for the assumed normal distribution monitored the effects of errors in the finite element solution.

Both the "weakest link" and series-parallel system are evaluated for desirability in estimating structural reliability. The weakest link approach, which introduces reliability independence between elements, will thereby describe a much more conservative reliability estimate than the series-parallel system which requires at least two adjacent elements to fail in order to have structural failure.

Examining the reliability computation for both structures as a function of assumed minimum detectable crack sizes indicated the importance of determining relatively small cracks to obtain acceptable reliability.

CONTENTS

	Page
INTRODUCTION.	1
TYPES OF STRUCTURES CONSIDERED.	2
STATISTIC EVALUATION OF VARIABLE STRENGTH	3
CONVENTIONAL FRACTURE MECHANICS APPROACH TO STRUCTURAL RELIABILITY. . .	4
FLAW SIMULATION METHOD.	5
STRUCTURAL STRESS ANALYSIS.	8
ELEMENT RELIABILITY CALCULATION METHODS	8
STRUCTURAL RELIABILITY.	9
NUMERICAL RESULTS AND DISCUSSION.	10
CONCLUSIONS	12
ACKNOWLEDGMENT.	13
APPENDIX A. PROBABILITY OF SURVIVAL DETERMINATION.	14
APPENDIX B. PROBABILITY OF ELEMENT SURVIVAL.	14
APPENDIX C. SERIES-PARALLEL CONCEPT (TENSION-COMPRESSION).	14

INTRODUCTION

Present linear elastic fracture mechanics (LEFM) procedures as applied to structural reliability depend on determination of critical crack sizes by using proper K_{IC} (fracture toughness) relationships in conjunction with known stress distributions in the structure.¹ In obtaining critical size, it is assumed the cracks are orientated normal to the maximum principal stress. Once the critical crack sizes and locations are established, a non-destructive test (NDT) procedure is applied to the structure to determine if this crack exists. If a critical crack is located, the structure is rejected. It should be noted that an excessively large rejection rate can occur by applying this method since the probability of the assumed crack orientation is very small.² Another objection to the LEFM procedure is the inability of NDT methods to detect cracks less than a certain size (e.g., 0.10 inch).^{*} If the critical size is computed to be less than this size then the LEFM procedure may not be able to determine potential failure in the structure.

The uncertainties existing in the use of the analytic tools, such as finite element (FE) analysis, in obtaining the structural stress distribution can introduce considerable error in obtaining the critical flaw size. For example, the accuracy of the FE solution depends on the severity of stress gradients, mesh size, types of elements used, and the effects of averaging stresses within the element. Therefore, it is important to recognize element stress variability in establishing structural reliability.

The flaw simulation scheme (FSS) introduced in this paper attempts to provide alternatives to the conventional methods described above. The FSS procedure does not describe exact reliability numbers but rather determines the effects of flaw detection capabilities and stress computation errors. Applying this sensitivity analysis also determines which possible parametric errors most affect the reliability computations. For example, if K_{IC} numbers obtained from laboratory test results indicated a 15 percent coefficient of variation (CV) and the resultant reliability computation was 0.850 versus 0.999 for an assumed CV of 5 percent, then one should attempt to reduce the variability in this parameter.

In using the Monte Carlo method,³ the flaw simulation scheme provides for variations in crack orientation and size in addition to computed stress values in the structure. Crack orientations are assumed to vary from 0° to 90° in a uniform random manner. The crack size variation is defined in exponential functional form where size varies from a large number of very small cracks to a relatively small number of larger detectable cracks.[†] The types of cracks and their locations are the through-center crack, near cut-out edge, corner crack, and surface crack (center). The structural configuration determines the types of cracks and their locations.

The stress values obtained for a cracked structural element is assumed to be a normal distribution where the CV is varied in order to determine the effect of errors in the FE analysis.

*HASTINGS, C. H. Army Materials and Mechanics Research Center, Watertown, Massachusetts, NDT Industrial Applications Branch, Personal Communication.

†SMITH, J. M. Army Materials and Mechanics Research Center, Watertown, Massachusetts, NDT Industrial Applications Branch, Personal Communication.

1. BLUHM, J. I., and FREESE, C. E. *Crack Inspection Maps - An Application to Copperhead*. Presented at the Army Symposium on Solid Mechanics, Bass River, Massachusetts, 3-5 October 1978; also Army Materials and Mechanics Research Center, AMMRC MS 78-3, October 1978, p. 307-319.
2. TETELMAN, A. S., and BESUNER, P. M. *The Application of Risk Analysis to the Brittle Fracture and Fatigue of Steel Structures*. Proceedings of the Fourth International Conference on Fracture, Pergamon Press, New York, v. 1, June 1977, p. 137-156.
3. SHREIDER, Y. A. *The Monte Carlo Method*. International Series of Monographs in Pure and Applied Mathematics, Pergamon Press, New York, v. 87, 1967.

The FE code used in obtaining stress values utilizes an 8-noded isoparametric element with substructuring capabilities. Each element contains 16 degrees of freedom with the complete structure represented by a minimum of 3000 degrees of freedom. In the substructuring procedure, the stiffness matrix solutions are modified in the reduction process to provide selected independent determination of the displacement coefficients.

The loading conditions applied to the structures used in demonstrating the applicability of the FSS are only approximations. Therefore, one should not assume any level of quality assurance of either the fragmentation shell or the antitank projectile (ATP).

TYPES OF STRUCTURES CONSIDERED

The model problems chosen to illustrate the technique proposed in this paper are the determination of structure reliability for the ATP control section (Figure 1) and a fragmentation shell (Figure 2). Both structures are made from relatively high strength, brittle steels. The projectile control section is subjected to relatively large compressive loads at the aft section and tensile stresses in the vicinity of the cut-out region where the fins are attached. The fragmentation shell is internally loaded with a uniform pressure of 14 ksi. This load represents a proof test used in evaluating shell quality. Reliability determination of the control section provided the opportunity to evaluate the series-parallel system approach because of the complex stress state introduced by the relatively large tension and compressive stresses in the structure. The weakest link approach is more readily adapted to the fragmentation shell loading state.

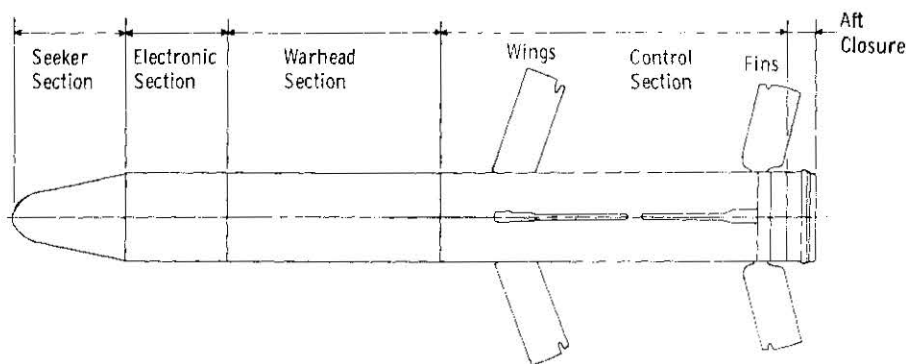


Figure 1. Antitank projectile configuration.

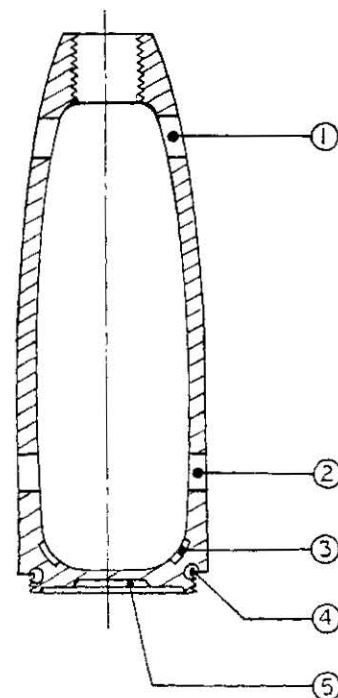


Figure 2. Cross-sectional view of fragmentation shell. (1) Ogive, (2) Bourrelet, (3) Inside Radius, (4) Thread Relief, and (5) Rear of Base.

STATISTIC EVALUATION OF VARIABLE STRENGTH

The lack of ductility characteristic of brittle materials has two undesirable consequences for the engineer. First, any misfit or misalignment produces locally high stresses which cannot be relieved by plastic flow, unlike ductile materials. Brittle component designs differ from those for similar ductile components in that extra attention must be paid to detail, especially in highly stressed areas. The second consequence is more fundamental; all materials contain flaws such as microscopic cavities and dislocations. In loaded brittle materials, these flaws result in local stress concentration within the material. The strength of a component is governed by the chance that a severe stress concentration (c) will be subjected to a stress (σ) such that the local stress $c\sigma$ exceeds the material strength. The occurrence of this is a matter of chance and explains the marked variability generally observed in brittle material strengths. It also explains why brittle material failures may start away from the maximum stress, and failure may occur at a severe flaw subject to a lower stress at a position where $c\sigma$ is a maximum.

To overcome the strength variability by drastically reducing the applied loading is not an attractive engineering proposition. What is needed is an estimate of the likelihood of failure of the component under a specified load. This requires a detailed knowledge of the stresses in the structure and the flaw distribution in the material. Well-established techniques are available for the stress analysis, some of which are mentioned later. The variation in material strength due to flaws in a particular material can be illustrated by fracture tests on a sample of specimens. A histogram of the fracture stresses of both brittle and ductile material subjected to uniform tension is shown in Figure 3a; the frequency of failure (F_f) is the fraction of the sample failing within the stress range σ to $\sigma + \delta\sigma$. In the limit, as the number of specimens (N) becomes large, the stress interval ($\delta\sigma$) in Figure 3b can be reduced to

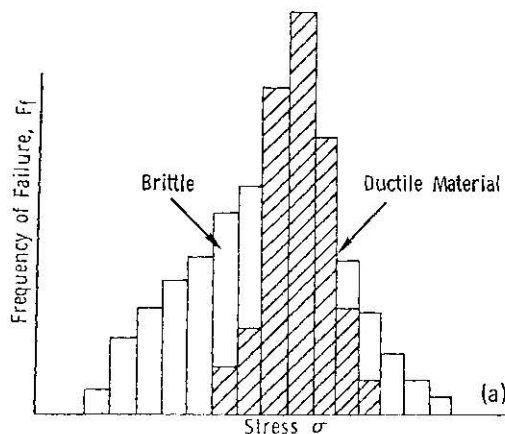
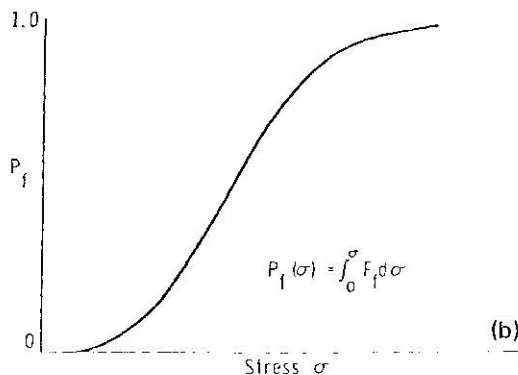


Figure 3. Probability of failure distribution.



give a continuous distribution curve. Note the relatively large variation in strength of the brittle material as compared to the corresponding ductile material of similar test specimens. Structures with large variations in material strength, as shown for the brittle material strength, require a probabilistic approach in the design procedures.

A complementary form of Figure 3a is obtained if the data is presented in terms of the cumulative failure probability (P_f). This quantity is the fraction of the sample failing at or below the stress σ ; in the limit it is the integral of the frequency distribution with respect to stress, i.e.,

$$P_f(\sigma) = \int_0^{\sigma} F_f d\sigma. \quad (1)$$

In practice, the estimated cumulative failure probability is usually found from the data using the "mean ranking" approach. The N failure stresses of the sample are arranged in ascending order: the cumulative failure probability associated with the i^{th} failure stress in the list is

$$P_f(\sigma_i) = i/N+1. \quad (2)$$

The probability distribution of the data can be plotted from this (see Figure 3b).

CONVENTIONAL FRACTURE MECHANICS APPROACH TO STRUCTURAL RELIABILITY

Fracture mechanics in the design process requires the consideration of three factors: a stress analysis, a measure of K_{IC} , and the capability of inspecting for cracks. The stress analysis can require elaborate analysis using advanced FE or simpler closed form solutions depending on loading conditions and structural geometry. Determinations of the plane strain fracture toughness of a material are necessary under a sufficiently wide variety of conditions to allow realistic assessment of the minimum range of values likely to be encountered in design conditions. Some of the crack detection techniques include ultrasonics, dye penetrants, magnetic particles, and visual inspection.

Analytically, the critical flaw size is defined by an expression of the type shown below:

$$a_c = f(Q, K_{IC}, \sigma) \quad (3)$$

Where: a_c = critical flaw depth,

Q = a parameter which takes into account the shape of the flaw,

K_{IC} = plane strain fracture toughness of the material, and

σ = the tensile component of stress acting normal to the plane of the flaw.

The critical flaw depth, on the basis of the fracture toughness and stress factors, can result in catastrophic crack propagation. It should be noted that σ , as defined above, assumes the flaw is normal to the acting stress (see Figure 4). This assumption rejects the possibility that the flaw could be oriented in other directions, thereby neglecting obvious possibilities in favor of an unlikely one. This could result in incorrectly determining critical flaw size a_c . Present flaw detection methods in many instances are not capable of detecting critical flaws of a relatively small size. In

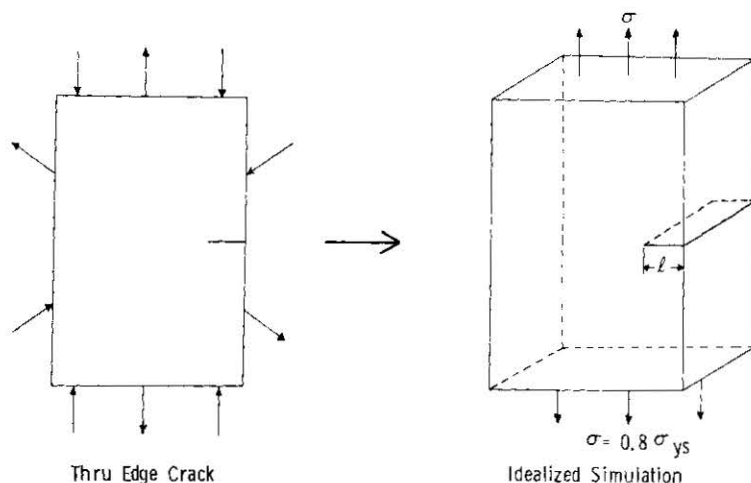


Figure 4. Conventional single-valued crack orientation.

fact, comments by Hastings indicate flaws less than 0.1 inch may not be found in a structure. Of course, the other difficulties involve not being able to find a detectable flaw in a structure although it does exist.

FLAW SIMULATION METHOD

An alternative to the previously described conventional fracture mechanics approach is made by introducing variation in crack orientation and length by means of the Monte Carlo method. Initially, four types of cracks are to be considered in an element (see Figure 5). The type and location of cracks depends on the structural configuration.

In the simulation scheme the allowable uniform stress σ from K_{IC} relationships is written as:

$$\sigma_c = f(K_{IC}, l, \theta) \quad (4)$$

where: l = crack length and

θ = angle of inclination of crack (see Figure 6d).

It is assumed that σ_c represents the material strength and depends on the parameters K_{IC} , l , θ . The variations in K_{IC} are represented by a normal probability density function (PDF) (Figure 6a). The angle θ is represented by uniform random numbers in the range of 0° to 90° (Figure 6b). The distribution of sizes θ is of an exponential PDF form shown in Figure 6c. The σ_c distribution is obtained from generating a set of uniform numbers and solving for x in the relation,

$$\int_{-\infty}^x f_i = R, \quad (5)$$

where R = uniform random number and f_i corresponds to the desired type of frequency distribution. The K_{IC} distribution requires test results for the material used in the structure in order to obtain the necessary mean and standard deviation values. In Figure 6c, the maximum crack length l_2 is represented by the smallest detectable crack consistent with the capability of presently available NDT methods. The assumed distribution of crack sizes has been substantiated by McClintock⁴ and Smith.*

*SMITH, J. M. Army Materials and Mechanics Research Center, Watertown, Massachusetts, NDT Industrial Applications Branch, Personal Communication.

4. MCCLINTOCK, F. A. *Statistics of Brittle Fracture*. Fracture Mechanics of Ceramics, v. 1, Plenum Press, New York, 1973, p. 93-114.

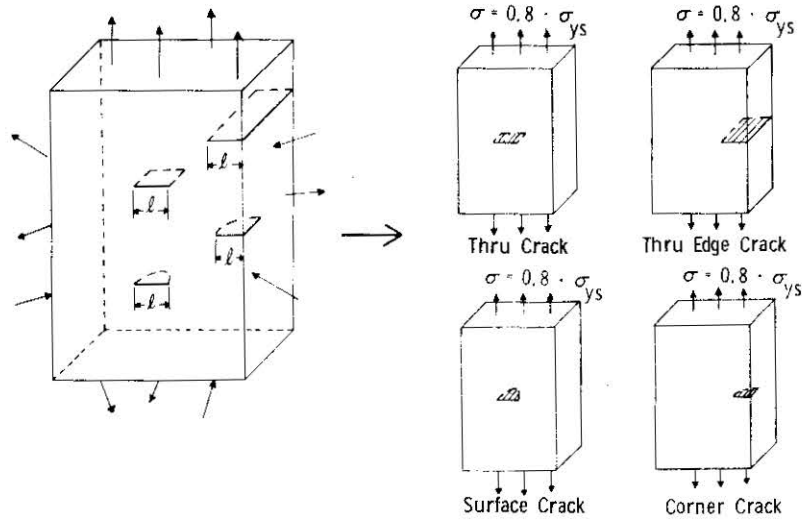


Figure 5. Crack types assumed in simulation scheme.

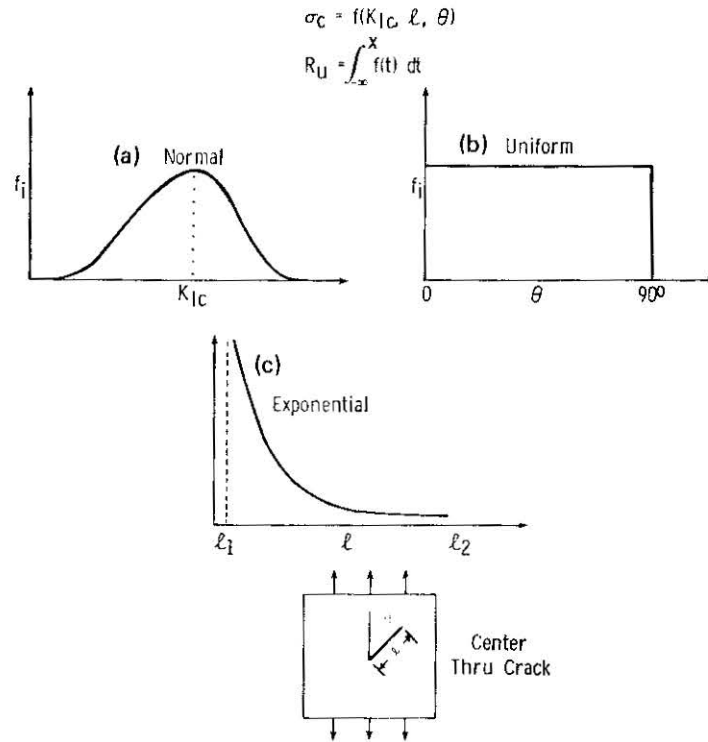


Figure 6. Simulation method.

A PDF can be obtained for the allowable stress σ_c by randomly selecting from K_{Ic} , θ and ℓ distributions discrete sets of numbers and substituting them into Equation 4. Note, there should be an equal amount of N random numbers for each parameter to have N numbers representing the σ_c distribution.

The K_{IC} relationships for σ_c are written as:

(a) Through crack

$$\sigma_c = K_{IC} (2/\pi)^{1/2} (\ell \sin^2 \theta)^{-1/2}$$

where:

$$K_{IC} = (K_I^2 + K_{II}^2)^{1/2}, \quad (6)$$

$$K_I = \sigma (\ell \pi / 2)^{1/2} \sin^2 \theta, \text{ and}$$

$$K_{II} = \sigma (\ell \pi / 2)^{1/2} \sin \theta \cos \theta.$$

(b) Corner crack

$$\sigma_c = K_{IC} / (2(1.28) (\ell / \pi)^{1/2}). \quad (7)$$

(c) Surface crack

$$\sigma_c = K_{IC} / 1.1 (\pi a / Q)^{1/2}$$

where:

$$Q = E(K)^2 - 0.212 (\sigma / \sigma_{ys})^2,$$

$E(K)$ = complete elliptical integral of the second kind,

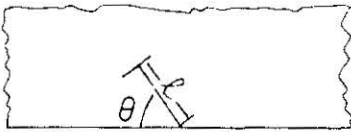
$$K^2 = 1 - (a/\ell)^2, \quad (8)$$

$$0 \leq a \leq 0.10 \text{ inch, and}$$

$$0 \leq \ell \leq 0.05 \text{ inch.}$$

The σ_c relationship for the inclined edge crack was obtained from application of a modified mapping collection scheme.* The results are presented in Table 1. The appropriate interpolation procedure was applied to use the Monte Carlo method as outlined in Equation 4.

Table 1. INCLINED EDGE CRACK SOLUTION



θ	$H_n = K_I / \sqrt{\pi \ell}$	$H_0 = K_{II} / \sqrt{\pi \ell}$
0	0.000	0.000
10	0.160	0.170
20	0.296	0.280
30	0.461	0.335
40	0.680	0.372
45	0.705	0.365
50	0.781	0.354
60	0.920	0.305
70	1.028	0.224
80	1.098	0.118
90	1.124	0.000

$$\sigma_c = K_{IC} / H_n \sqrt{\pi \ell}$$

*FREESE, C. E. Army Materials and Mechanics Research Center, Watertown, Massachusetts, unpublished results.

STRUCTURAL STRESS ANALYSIS

A finite element analysis was applied to obtain the stress distributions in the ATP and fragmentation shell. The loading consists of a set-back compressive load acting at the base of the ATP and an internal pressure (proof-test load) applied to the shell. Rectangular elements were used in the analysis for both structures where the shell contains 693 elements and the ATP contains 601 elements. The FE solution determines the average maximum and minimum principal stresses in each element. The maximum stress is used in the reliability determinations. These stresses should not be confused with critical stresses obtained from the K_{IC} relationships previously described. Having obtained the element stresses and corresponding σ_c or strength values, reliability of the elements can be determined.

ELEMENT RELIABILITY CALCULATION METHODS

Element reliability as related to the stress-strength (Warner) diagram⁵ method (see Appendix A) assumes that the probability of survival (reliability) is the probability that material strength will be greater than the stress in a given structural element over a range of stress values. The uncertainties in the FE solution are represented by a normal distribution f_2 , where the calculated mean stress and the assumed CV are the functional parameters. The distribution f_1 is obtained from known strength data (e.g., laboratory tests). This distribution does not necessarily have to be a normal function. It can be any PDF that accurately represents the empirical ranked data. In Appendix A, the probability of S_1 occurring is $f_2(S_1)$, while the probability of strength greater than S_1 is represented by the integral, with f_1 the integrand and limits of S_1 and Multiplication of these elements provides the necessary independence between the two conditions. Finally, integration over the entire range of stress values defines probability of survival P_s of each element.

Element reliability numbers were also obtained from an approach similar to the one previously described except that discrete values obtained from FSS were used to represent σ_c . Element design stress is normally represented in the same manner except distributed numbers are obtained from the new stress and assumed CV. This is a reasonable approach since distribution of strength values do not necessarily conform to any known density function. The tails of the two density functions are more accurately represented than by some crude approximating function. This method is outlined in Appendix B where the probability of element survival is defined as follows: $\alpha_i = 1$, when strength is greater than stress values, otherwise it is zero. This process is completed when all combinations are considered. The relationship P_{sK} therefore defines the Kth element reliability number.

The Weibull statistic was used for comparison purposes in obtaining element reliability of the fragmentation shell. This procedure is recommended for brittle materials subjected to the uniform tension state, which is consistent with the structural loads and material described for the shell. The Weibull⁶ PDF is commonly used in ceramics and other brittle materials evaluation. It employs the weakest link concept which is consistent with failure phenomenon of brittle materials subjected to tensile stresses primarily. A plot of strength versus cumulative density function (CDF) for HF-I steel used in the fragmentation shell construction is shown in Figure 7. Note the excellent correlation between empirical data and the Weibull function.

5. HAUGEN, E. B. *Probabilistic Approaches to Design*. John Wiley and Sons, Inc., New York, 1968.

6. WEIBULL, W. *A Static Theory of the Strength of Materials*. Proceedings of the Royal Swedish Academy of Engineering Sciences, v. 151, January 1939.

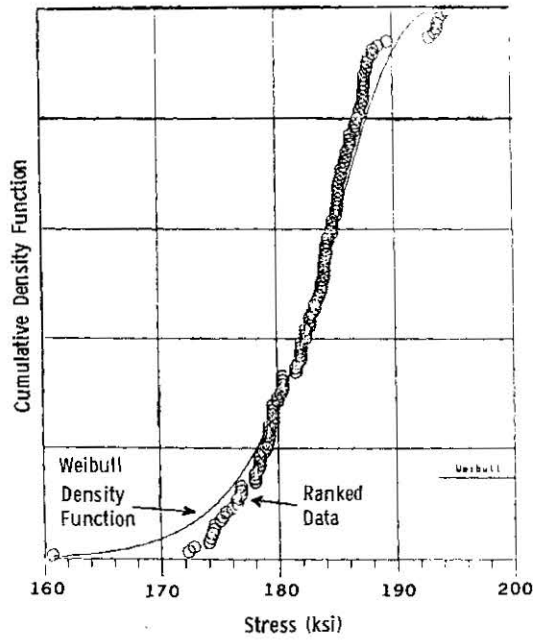


Figure 7. Cumulative density function versus stress.

The Weibull probability of survival P_{s_i} for individual stressed components is written as

$$P_{s_i} = \exp \left[\frac{-KV_i}{V^*} \left(\sigma_{\max_i} / \sigma_0 \right)^m \right] \quad (9)$$

where: $K = 1$ for simple tensile stress,
 V_i = volume of element,
 V^* = volume of test specimen,
 σ_{\max_i} = maximum principal stress in the element, and

σ_0 and m are functional parameters obtained from test data using the maximum likelihood method. It is obvious that P_{s_i} is volume dependent, that is, larger volume provides smaller P_{s_i} numbers.

STRUCTURAL RELIABILITY

In order to obtain P_s of the entire structure, the weakest link concept is applied, that is, it is assumed that each event or element probability of survival is independent of any other one in the structure. Therefore, the total P_s is written as

$$P_s = \prod_{K=1}^N P_{s_K}, \quad (10)$$

where: N = number of elements in the structure and
 P_{s_K} = the probability of survival of the individual element.

The corresponding probability of failure is defined as $P_f = 1 - P_s$.

A series-parallel approach is introduced to examine the case where more than one element is required to fail in order to have total structural failure. This method is described by examining a four-element structure where two elements must fail (see Appendix C). The P_{Si} values are determined for the elements by one of the methods previously described. The resultant P_S for the four elements is determined from application of the series approach. It should be noted that this method is somewhat less conservative than the conventional weakest link method. It is possibly more realistic, especially for the complex states that exist in the ATP structure.

NUMERICAL RESULTS AND DISCUSSION

Numerical reliability (R) results are listed in Table 2 for the fragmentation shell subjected to an internal pressure of 14 ksi (proof-test load) as a function of minimum detectable crack size. The Warner diagram method, as outlined in the text, is represented by normal stress-strength PDF's determined from FE solution and laboratory strength test results. The FSS results are obtained by applying the method presented in the text where the strength PDF is the result of using the simulation scheme (see Appendix B). The Weibull R values were obtained from application of Equation 9. It should be noted that both Warner and Weibull methods do not show variations due to changes in crack sizes. This is expected since they do not consider results from FSS procedures, which indicates the importance of finding a crack of at least 0.025 inch or less to establish at least 92% probability of survival. The Warner diagram shows an estimate of 1 failure in 1000, and the Weibull method shows an estimate of 222 failures in 1000. A coefficient of variation of 10% represents the variation in element stress values obtained from the finite element solution.

In Table 3, probability of survival estimates are given for variation in crack sizes of 0.020 inch. The effects of FE solution errors (e.g., CV values) are less than for larger cracks of 0.100 inch. Mean and CV values for K_{IC} were obtained from laboratory test data. The material yield strength of 140 ksi provided an upper bound for calculated σ_c (allowable stress) obtained from the FSS approach.

Table 4 provides a partial listing of reliability for the ATP system where crack sizes are 0.100 and 0.050 inch with variations in CV of 5% to 20%. The effects of FE errors are noted as in Table 3: small variation - better reliability; large variation - poorer reliability. The reliability numbers in parentheses are the results from application of the series-parallel method described in the text.

The series-parallel method which requires failure of all adjacent elements to have structural failure provides a much less conservative estimate of reliability. It is possible that an upper and lower bound on reliability of this structure for the specified crack sizes could be a series-parallel system and the weakest link approach, respectively. With tension and compressive stresses existing in this structure, it does not seem advisable to consider structural failure in terms of only one given element failure. It is also unreasonable to assume that all adjacent elements must fail to have structural failure, particularly if a bending stress exists in the structure.

Although the FSS model is an idealized method for estimating structural reliability, it does provide a desirable alternative to the present fracture mechanics approach which assumes cracks are orientated transverse to the maximum principal stress, resulting in unnecessarily high rejection rates. The ability to examine, at least qualitatively, the reliability of structures as related to the ability to detect flaws

or cracks of various magnitudes can provide a guide for future NDT development procedures. If more information was known regarding structural flaw distributions, the FSS application could provide an excellent reliability tool, certainly one superior to the present laboratory test procedures applied to brittle materials. It should be noted that in laboratory testing, surface flaws are often removed from material thereby preventing an accurate representation of the material's strength as it is related to the structural component.

Table 2. RELIABILITY RESULTS VERSUS MINIMUM DETECTABLE CRACK SIZE

Minimum Detectable Crack Size (in.)	Probability of Survival - Shell (Proof-Test Load)		
	Warner Diagram	Monte Carlo (F.M.)	Weibull
0.100	0.999	0.059	0.778
0.050	0.999	0.451	0.778
0.025	0.999	0.920	0.778

CV (Element Stress) = 10%

$K_{IC} = 30 \text{ ksi}\sqrt{\text{in.}}$, CV = 12%

Yield Strength = 140 ksi

Table 3. STRUCTURAL RELIABILITY OF SHELL (PROOF-TEST CONDITION)

Minimum Detectable Crack Size (in.)	CV (Element Stress)			
	5%	10%	15%	20%
0.100	0.210	0.059	0.027	0.022
0.075	-	-	-	-
0.050	0.557	0.451	0.378	0.337
0.020	0.972	0.966	0.956	0.935
0.010	-	-	-	-

$K_{IC} = 30 \text{ ksi}\sqrt{\text{in.}}$, CV = 15%

Yield Strength = 160 ksi

Table 4. STRUCTURAL RELIABILITY OF ATP SYSTEM

CV (Element Stress) Crack Size (in.)	5%	10%	15%	20%
0.100	0.353 (0.960)	0.152 (0.841)	0.079 (0.744)	0.042 (0.569)
0.075	-	-	-	-
0.050	0.606 (0.976)	0.450 (0.970)	0.378 (0.965)	0.325 (0.954)
0.025	-	-	-	-

$K_{IC} = 40 \text{ ksi}\sqrt{\text{in.}}$, CV = 10%

Yield Strength = 215 Tension, Yield Strength = 240 Compression

Numbers in parentheses are series-parallel systems; others, weakest link concept.

In application of the FSS, determination of the proper number of simulations in the Monte Carlo method was obtained from examining the convergence rate for the calculated reliability numbers. Instead of relying on some elaborate formulation for establishing the proper number of simulations, a chart similar to the one shown in Figure 8 was used. All functional parameters were increased equally in number to examine all effects of the simulation. To examine the acceptability of this method, a comparison was made for R using the Warner diagram approach where normal PDF's were calculated from a prescribed mean and standard deviation to represent the stress-strength values. Results show excellent agreement with the FSS simulation method, using the convergence criteria for number of simulations (see Figure 8).

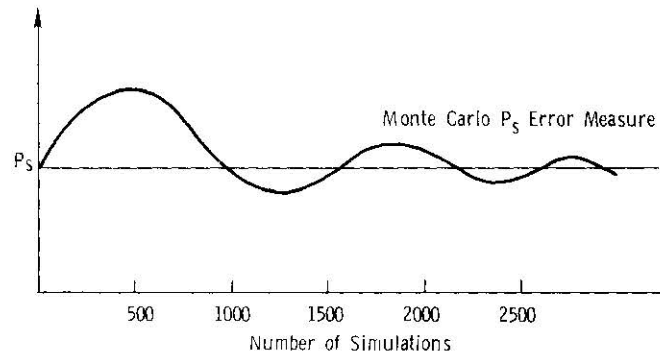


Figure 8.

CONCLUSIONS

The flaw simulation scheme requires that each structural element contain an isolated flaw of a particular geometry. This assumption introduces an idealization which somewhat limits acceptability of the quantitative results presented. Although these limitations exist, it has been demonstrated that application of this scheme can provide a sensitivity analysis in relation to flaw detection capabilities as noted in Tables 2, 3, and 4.

The Warner diagram and Weibull approach provide a means of obtaining structural reliability without application of the conventional fractural mechanics methodology. These methods can provide either too conservative or overly optimistic (e.g., Warner diagram) reliability results as demonstrated in Table 2.

The weakest link and series-parallel schemes are reasonable computational methods for obtaining reliability error bounds as related to structural failure mechanisms. As noted in Table 4, the weakest link approach represents the lower bound (conservative estimate) while series-parallel determines the upper bound. The latter is probably more realistic for the ATP system with the other more applicable for shell reliability computations.

The effects of increasing uncertainties in application of the FE solution are demonstrated from the results in Tables 3 and 4. The results in both tables indicate a reduction in reliability, with the amount of decrease depending on the detectable crack size.

It is obvious from the tabulated results that in order to have acceptable reliability of the structures, one should be able to determine relatively small size cracks (e.g., 0.025 inch or less).

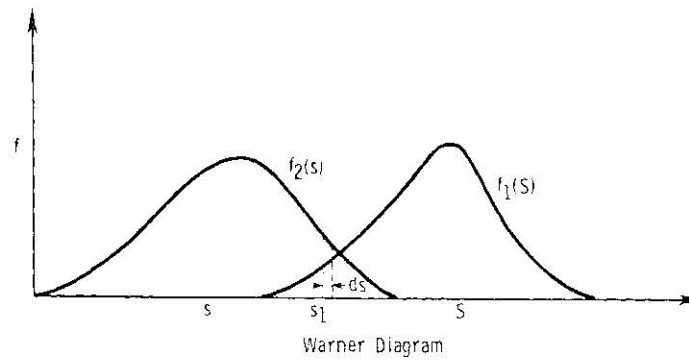
The primary contribution of the flaw simulation scheme is the ability to isolate the effects of the various parameters involved in determining structural reliability from a LEFM technology. The ability to recognize excessive reduction in reliability due to relatively small errors in the parameter can establish need for improvement in the parametric determination. Accurate quantitative reliability values are extremely difficult to predict; therefore, the objective should be to reduce the error in the prediction process by making necessary improvements in the sensitive parameter determinations.

The failure rate reported by the fragmentation shell manufacturer during proof testing was from 2 to 5 percent depending on the production lot. Since shells containing flaws greater than 0.020 in. were rejected prior to proof testing, this result correlates exceptionally well with the results shown in Table 3. Although the objective of the paper was to obtain a sensitivity analysis with respect to the critical stress parameters, the results have indicated possible quantitative acceptance of the FSS reliability computations.

ACKNOWLEDGMENT

The authors acknowledge the support from Joseph I. Bluhm for providing inspiration and guidance.

APPENDIX A. PROBABILITY OF SURVIVAL DETERMINATION



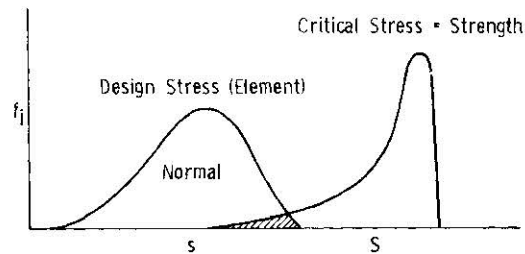
s = Calculated Stress
 S = Materials Strength

$$dP_s = f_2(s_1) ds \int_{s_1}^{\infty} f_1(S) dS$$

$$\text{And } P_s = \int dP_s = \int_{-\infty}^{\infty} f_2(s) \left[\int_s^{\infty} f_1(S) dS \right] ds$$

Where $f(s)$ and $f(S)$ are PDF representation for stress and strength values respectively.

APPENDIX B. PROBABILITY OF ELEMENT SURVIVAL



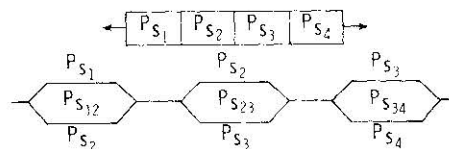
$$P_{SK} = 1/M^2 \sum_{j=1}^M \sum_{i=1}^M \alpha_i \quad \text{where } \alpha_i = \begin{cases} 1, & S_i > s_j \\ 0 & \text{Otherwise} \end{cases}$$

M = Number Simulations

P_{SK} = Probability of Survival of Element K

APPENDIX C. SERIES-PARALLEL CONCEPT (TENSION-COMPRESSION)

Assume simply four element structure



$$\text{e.g., } P_{S12} = P_{S1} + P_{S2} - P_{S1} \cdot P_{S2}$$

Survival Probability for Structure

$$P_S = P_{S12} \cdot P_{S23} \cdot P_{S34}$$

For large structures all elements are considered with their corresponding adjacent elements.

DISTRIBUTION LIST

No. of Copies	To
1	Office of the Under Secretary of Defense for Research and Engineering, The Pentagon, Washington, DC 20301
12	Commander, Defense Technical Information Center, Cameron Station, Building 5, 5010 Duke Street, Alexandria, VA 22314
1	Metals and Ceramics Information Center, Battelle Columbus Laboratories, 505 King Avenue, Columbus, OH 43201
1	Deputy Chief of Staff, Research, Development, and Acquisition, Headquarters Department of the Army, Washington, DC 20310
1	ATTN: DAMA-ARZ
1	Commander, Army Research Office, P.O. Box 12211, Research Triangle Park, NC 27709
1	ATTN: Information Processing Office
1	Dr. F. W. Schmiedeshoff
1	Commander, U. S. Army Materiel Development and Readiness Command, 5001 Eisenhower Avenue, Alexandria, VA 22333
1	ATTN: DRCLDC
1	Commander, U. S. Army Materiel Systems Analysis Activity, Aberdeen Proving Ground, MD 21005
1	ATTN: DRXSY-MP, H. Cohen
1	Commander, U.S. Army Communications-Electronics Command, Fort Monmouth, NJ 07703
1	ATTN: DRSEL-LE-R
1	Commander, U. S. Army Missile Command, Redstone, AL 35809
1	ATTN: DRSMI-RRP, J. Wright, Bldg. 7574
1	DRSMI-TB, Redstone Scientific Information Center
1	DRSMI-RLM
1	Commander, U. S. Army Natick Research and Development Laboratories, Natick, MA 01760
1	ATTN: Technical Library
1	Dr. E. W. Ross
1	DRDNA-UE, Dr. L. A. McClaine
1	Commander, U.S. Army Satellite Communications Agency, Fort Monmouth, NJ 07703
1	ATTN: Technical Document Center
1	Commander, U.S. Army Tank-Automotive Research and Development Command, Warren, MI 48090
1	ATTN: DRDTA-RKA
1	DRDTA-UL, Technical Library
1	Commander, U.S. Army Armament Research and Development Command, Dover, NJ 07801
2	ATTN: DRDAR-TSS, Technical Library
1	DRDAR-SCM, J. D. Corrie
1	DRDAR-LC, Dr. J. Fraiser
1	DRDAR-LCA, Mr. Harry E. Peibly, Jr., PLASTECH, Director
1	DRDAR-LCA, Mr. J. Pearson
1	DRDAR-LCA, G. Randers-Pehrson
1	DRDAR-LCA, Mr. A. Garcia
1	George Demitrak
1	Mr. S. Nicolaides
1	Commander, White Sands Missile Range, NM 88002
1	ATTN: STEWS-WS-VT
1	Commander, U.S. Army Armament Research and Development Command, Aberdeen Proving Ground, MD 21010
1	ATTN: DRDAR-QAC-E
1	Director, U.S. Army Ballistic Research Laboratory, Aberdeen Proving Ground, MD 21005
1	ATTN: Dr. R. Vitali
1	Dr. G. L. Filbey
1	Dr. W. Gillich
1	DRDAR-TSB-S (STINFO)
1	Mr. A. Elder
1	Commander, Harry Diamond Laboratories, 2800 Powder Mill Road, Adelphi, MD 20783
1	ATTN: Technical Information Office

No. of Copies	To
1	Commander, Watervliet Arsenal, Watervliet, NY 12189
1	ATTN: DRDAR-LCB, Dr. T. Davidson
1	DRDAR-LCB, Mr. D. P. Kendall
1	DRDAR-LCB, Mr. J. F. Throop
1	DRDAR-LCB-TL, Mr. V. Vrooman
1	Commander, U.S. Army Foreign Science and Technology Center, 220 7th Street, N.E. Charlottesville, VA 22901
1	ATTN: Mr. Marley, Military Tech
1	Director, Eustis Directorate, U.S. Army Air Mobility Research and Development Laboratory, Fort Eustis, VA 23604
1	ATTN: Mr. J. Robinson, DAVDL-E-MOS (AVRADCOM)
1	U.S. Army Aviation Training Library, Fort Rucker, AL 36360
1	ATTN: Building 5906-5907
1	Commander, U.S. Army Agency for Aviation Safety, Fort Rucker, AL 36362
1	ATTN: Librarian, Bldg. 4905
1	Commander, USACDC Air Defense Agency, Fort Bliss, TX 79916
1	ATTN: Technical Library
1	Commander, U.S. Army Engineer School, Fort Belvoir, VA 22060
1	ATTN: Library
1	Commander, U.S. Army Engineer Waterways Experiment Station, Vicksburg, MS 39180
1	ATTN: Research Center Library
1	Commander, U. S. Army Research and Technology Laboratory, Air Mobility Research and Development Laboratory, Ames Research Center, Moffett Field, CA 94035
1	ATTN: Dr. R. Foye
1	Commander, Naval Air Engineering Center, Lakehurst, NJ 08733
1	ATTN: Technical Library, Code 1115
1	Commander, U.S. Army Aviation Research and Development Command, 4300 Goodfellow Boulevard, St. Louis, MO 63120
1	ATTN: DRDAV-EQA, Philip J. Haselbauer
1	Director, Structural Mechanics Research, Office of Naval Research, 800 North Quincy Street, Arlington, VA 22203
1	ATTN: Dr. N. Perrone
1	David W. Taylor Naval Ship Research and Development Center, Annapolis, MD 21402
1	ATTN: Dr. H. P. Chu
1	Naval Research Laboratory, Washington, DC 20375
1	ATTN: C. D. Beachem, Head, Adv. Mat'l's Tech Br. (Code 6310)
1	Dr. J. M. Krafft - Code 5830
1	E. A. Lange
1	Dr. P. P. Puzak
1	R. J. Sanford - Code 8436
1	A. M. Sullivan
1	R. W. Rice
1	S. W. Freiman
1	Dr. Jim C. L. Chang
1	Chief of Naval Research, Arlington, VA 22217
1	ATTN: Code 471
1	Naval Weapons Laboratory, Washington, DC 20390
1	ATTN: H. W. Romine, Mail Stop 103
1	Ship Research Committee, Maritime Transportation Research Board, National Research Council, 2101 Constitution Avenue, N.W., Washington, DC 20418
1	Commander, U.S. Air Force Wright Aeronautical Laboratories, Wright-Patterson Air Force Base, OH 45433
2	ATTN: AFWAL/MLSE, E. Morrissey
1	AFWAL/MLC
1	AFWAL/MLLP, D. M. Forney, Jr.
1	AFWAL/MLBC, Mr. Stanley Schulman
1	AFWAL/MLNC, T. J. Reinhart
1	AFWAL/FR, Dr. J. C. Halpin

No. of Copies	To
	Air Force Flight Dynamics Laboratory, Wright-Patterson Air Force Base, OH 45433
1	ATTN: AFFDL (FBS), C. Wallace
1	AFFDL (FRE), C. D. Sundecky
	National Aeronautics and Space Administration, Washington, DC 20546
1	ATTN: Mr. B. C. Achhammer
1	Mr. G. C. Deutsch - Code RW
	National Aeronautics and Space Administration, Marshall Space Flight Center, Huntsville, AL 35812
1	ATTN: R. J. Schwinghammer, EH01, Dir., M&P Lab
1	Mr. W. A. Wilson, EH41, Bldg. 4612
	National Aeronautics and Space Administration, Langley Research Center, Hampton, VA 23665
1	ATTN: Mr. H. F. Hardrath, Mail Stop 188M
1	Dr. R. J. Hayduck, Mail Stop 243
	National Aeronautics and Space Administration, Lewis Research Center, 21000 Brookpark Road, Cleveland, OH 44135
1	ATTN: Dr. J. E. Srawley, Mail Stop 105-1
1	Mr. W. F. Brown, Jr.
1	Mr. M. H. Hirschberg, Head, Fatigue Research Section, Mail Stop 49-1
1	Mr. R. F. Lark, Mail Stop 49-3
	Lockheed-Georgia Company, 86 South Cobb Drive, Marietta, GA 30063
1	ATTN: Materials and Processes, Eng. Dept., 71-11, Zone 54
	National Bureau of Standards, U.S. Department of Commerce, Washington, DC 20234
1	ATTN: Mr. J. A. Bennett
1	Mechanical Properties Data Center, Belfour Stulen Inc., 1391/ W. Bay Shore Drive, Traverse City, MI 49684
	Midwest Research Institute, 425 Coker Boulevard, Kansas City, MO 64110
1	ATTN: Mr. G. Gross
	Southwest Research Institute, 8500 Culebra Road, San Antonio, TX 78284
1	ATTN: Dr. W. Baker
1	Mr. J. G. Kaufman, Alcoa Research Laboratories, New Kensington, PA 15068
1	Mr. P. N. Randall, TRW Systems Group - 0-1/2210, One Space Park, Redondo Beach, CA 90278
1	Dr. E. A. Steigerwald, TRW Metals Division, P.O. Box 250, Minerva, OH 44657
1	Dr. George R. Irwin, Department of Mechanical Engineering, University of Maryland, College Park, MD 20742
1	Mr. W. A. Van der Sluys, Research Center, Babcock and Wilcox, Alliance, OH 44601
1	Mr. B. M. Wundt, 2346 Shirl Lane, Schenectady, NY 12309
	Battelle Columbus Laboratories, 505 King Avenue, Columbus, OH 43201
1	ATTN: Mr. J. Campbell
1	R. G. Hoagland, Metal Science Group
	General Electric Company, Schenectady, NY 12010
1	ATTN: Mr. A. J. Brothers, Materials & Processes Laboratory
	General Electric Company, Schenectady, NY 12309
1	ATTN: Mr. S. Yukawa, Metallurgy Unit
1	Mr. F. E. Zwicky, Jr.
	General Electric Company, Knolls Atomic Power Laboratory, P.O. Box 1072, Schenectady, NY 12301
1	ATTN: Mr. F. J. Mehringer
1	Dr. L. F. Coffin, Room IC41-K1, Corp. R&D, General Electric Company, P.O. Box 8, Schenectady, NY 12301
	United States Steel Corporation, Monroeville, PA 15146
1	ATTN: Mr. S. R. Novak
1	Dr. A. K. Shoemaker, Research Laboratory, Mail Stop 78

No. of Copies	To
	Westinghouse Electric Company, Bettis Atomic Power Laboratory, P.O. Box 109, West Mifflin, PA 15122
1	ATTN: Mr. R. G. Hoppe, Manager
	Westinghouse Research and Development Center, 1310 Beulah Road, Pittsburgh, PA 15235
1	ATTN: Mr. E. T. Wessel
1	Mr. M. J. Manjoine
	Brown University, Providence, RI 02912
1	ATTN: Prof. J. R. Rice
1	Prof. W. N. Findley, Division of Engineering, Box D
	Carnegie-Mellon University, Department of Mechanical Engineering, Schenley Park, Pittsburgh, PA 15213
1	ATTN: Dr. J. L. Swedlow
1	Prof. J. D. Lubahn, Colorado School of Mines, Golden, CO 80401
1	Prof. J. Dvorak, Civil Engineering Department, University of Utah, Salt Lake City, UT 84112
1	Prof. E. Rybicki, Chairman, Mech. Eng. Dept., University of Tulsa, Tulsa, OK 74104
	George Washington University, School of Engineering and Applied Sciences, Washington, DC 20052
1	ATTN: Dr. H. Liebowitz
	Lehigh University, Bethlehem, PA 18015
1	ATTN: Prof. C. C. Sih
1	Prof. R. Roberts
1	Prof. R. P. Wei
1	Prof. F. Erodgan
	Terra Tek, University Research Park, 420 Wakara Way, Salt Lake City, UT 84108
1	ATTN: Dr. A. Jones
1	Librarian, Materials Sciences Corporation, Blue Bell Office Campus, Merion Towle House, Blue Bell, PA 19422
	Massachusetts Institute of Technology, Cambridge, MA 02139
1	ATTN: Prof. B. L. Averbach, Materials Center, 13-5082
1	Prof. F. A. McClintock, Room 1-304
1	Prof. R. M. Pelloux
1	Prof. T. H. H. Pian, Department of Aeronautics and Astronautics
1	Prof. A. S. Argon, Room 1-306
1	Prof. J. N. Rossettos, Department of Mechanical Engineering, Northeastern University, Boston, MA 02115
1	Prof. R. Greif, Department of Mechanical Engineering, Tufts University, Medford, MA 02155
1	Dr. D. E. Johnson, AVCO Systems Division, Wilmington, MA 01887
	University of Delaware, Department of Aerospace and Mechanical Engineering, Newark, DE 19711
1	ATTN: Prof. B. Pipes
1	Prof. J. Vinson
	Syracuse University, Department of Chemical Engineering and Metallurgy, 409 Link Hall, Syracuse, NY 13210
1	ATTN: Mr. H. W. Liu
1	Dr. V. Weiss, Metallurgical Research Labs., Bldg. D-6
	FAA, 800 Independence Avenue, S.W., Washington, DC 20591
1	ATTN: Joseph Soderquist, Aws-102
	Ames Laboratory, Energy and Mineral Resources Research Institute, Iowa State University, Ames, IA 50011
1	ATTN: Loren W. Zachary
	Boeing Company, Box 3707, MS 30-01, Seattle, WA 98124
1	ATTN: Ray E. Horton
	Stanford Research Institute International, 333 Ravenswood Avenue, Menlo Park, CA 94025
1	ATTN: Dr. D. Shockey
1	Dr. D. Curran
1	Dr. L. Seaman

No. of Copies	To
	Harvard University, Div. of Applied Sciences, Oxford Street, Cambridge, MA 02138
1	ATTN: Prof. J. Hutchinson
1	Prof. J. Rice
1	Prof. E. R. Parker, Department of Materials Science and Engineering, University of California, Berkeley, CA 94700
1	Prof. W. Goldsmith, Department of Mechanical Engineering, University of California, Berkeley, CA 94720
	University of California, Los Alamos Scientific Laboratory, Los Alamos, NM 87544
1	ATTN: Dr. R. Karp
1	Prof. A. J. McEvily, Metallurgy Department U-136, University of Connecticut, Storrs, CT 06268
1	Prof. D. Drucker, Dean of School of Engineering, University of Illinois, Champaign, IL 61820
	University of Illinois, Urbana, IL 61801
1	ATTN: Prof. T. J. Dolan, Department of Theoretical and Applied Mechanics
1	Prof. J. Morrow, 321 Talbot Laboratory
1	Mr. G. M. Sinclair, Department of Theoretical and Applied Mechanics
1	Prof. R. I. Stephens, Materials Engineering Division, University of Iowa, Iowa City, IA 52242
1	Prof. D. K. Felbeck, Department of Mechanical Engineering, University of Michigan, 2046 East Engineering, Ann Arbor, MI 48109
1	Dr. M. L. Williams, Dean of Engineering, 240 Benedum Hall, University of Pittsburgh, Pittsburgh, PA 15260
1	Prof. A. Kobayashi, Department of Mechanical Engineering, FU-10, University of Washington, Seattle, WA 98195

No. of Copies	To
	State University of New York at Stony Brook, Stony Brook, NY 11790
1	ATTN: Prof. Fu-Pen Chiang, Department of Mechanics
	Denver Research Institute, 2390 South University Boulevard, Denver, CO 80210
1	ATTN: Dr. R. Recht
1	Dr. Robert S. Shane, Shane Associates, Inc., 7821 Carrleigh Parkway, Springfield, VA 22152
1	Prof. R. H. Gallagher, Dean of Engineering, University of Arizona, Tucson, AZ 85721
1	Dr. Z. Zudans, V. P. Engineering, The Franklin Institute, 20th and Parkway, Philadelphia, PA 19103
1	Dr. D. J. Ayres, 9487-421, Combustion Engineering Inc., Windsor, CT 06095
1	Dr. S. W. Key, Appl. Mech. I, Div. 5521, Sandia Laboratories, Albuquerque, NM 87115
1	Prof. T. J. R. Houghes, Div. of Appl. Mech., Stanford University, Stanford, CA 94305
1	Dr. D. S. Griffin, Struct. Mech. Dept., Advanced Reactor Div., Westinghouse Electric Corp., P.O. Box 158, Madison, PA 15663
1	Dr. T. U. Martsen, Electric Power Research Institute, P.O. Box 10412, Palo Alto, CA 94304
1	Mr. R. J. Zentner, EAI Corporation, 198 Thomas Johnson Drive, Suite 16, Frederick, MD 21701
	Director, Army Materials and Mechanics Research Center, Watertown, MA 02172
2	ATTN: DRXMR-PL
2	Authors